Evaluation of Biomechanics Associated with Muscle Spindle Afferent Firing

Faisal Reza, Dipta Paul, Supreeth Sai Krishna

New York University, Department of Biomedical Engineering

Abstract

Muscle spindles are essential sensory organs distributed throughout striated muscles, providing vital information to the central nervous system regarding muscle position and movement. They consist of intrafusal muscle fibers surrounded by extrafusal muscle fibers, with a complex network of sensory endings and motor neurons regulating their function. The dynamic interplay between muscle spindle biomechanics and neural control is critical for proprioception, motor coordination, and overall musculoskeletal health. The novel study presented focuses on how muscle spindle firing characteristics are influenced by intrafusal fiber force and yank during passive stretch conditions. By elucidating these relationships, the study seeks to contribute to the development of more accurate models and interventions for neuromuscular disorders and motor impairment. Researchers recorded muscle-tendon forces and muscle spindle afferent firing rates in experimentally anesthetized rats during passive stretch of the triceps surae muscles. They then developed a generative model based on simplified representations of intrafusal muscle mechanics, incorporating independent effects of alpha and gamma drive on muscle spindle firing. The computational model utilized a cross-bridge cycling model to simulate intrafusal muscle fiber mechanics, distinguishing between dynamic and static fibers analogous to bag_1 and bag_2 chain fibers. The model successfully predicted muscle spindle firing rates based on mechanical interactions within the muscle spindle and muscle-tendon unit. By simulating dynamic and static fibers' contributions to neural firing rates, the model replicated observed firing patterns during stretch trials. Despite the promising results, the study acknowledges several limitations. One major limitation is the model's inability to fully replicate all experimental responses, particularly the triangle responses observed in anesthetized rat models. Further refinement of the computational model includes incorporation of voltage-gated ion channels as well as addressing occlusion between bag_1 and bag_2 influence during initial and subsequent stretching. In conclusion, this study contributes to the ongoing efforts to unravel the complex interplay between muscle spindle biomechanics and neural control. By addressing the identified shortcomings and exploring future directions, researchers aim to develop more comprehensive models that advance our understanding of muscle spindle function and pave the way for improved interventions in neuromuscular disorders and motor impairment.

Keywords: Muscle spindle, muscle fiber, afferent firing, cross-bridge, biomechanics

Introduction

Background

Muscle spindles are sensory structures that keep the central nervous system updated about position and movement of body parts. Muscle spindles are present in most striated muscles, ranging from 1-100 spindles per gram of muscle, with the human body containing around 30,000 spindles [1].

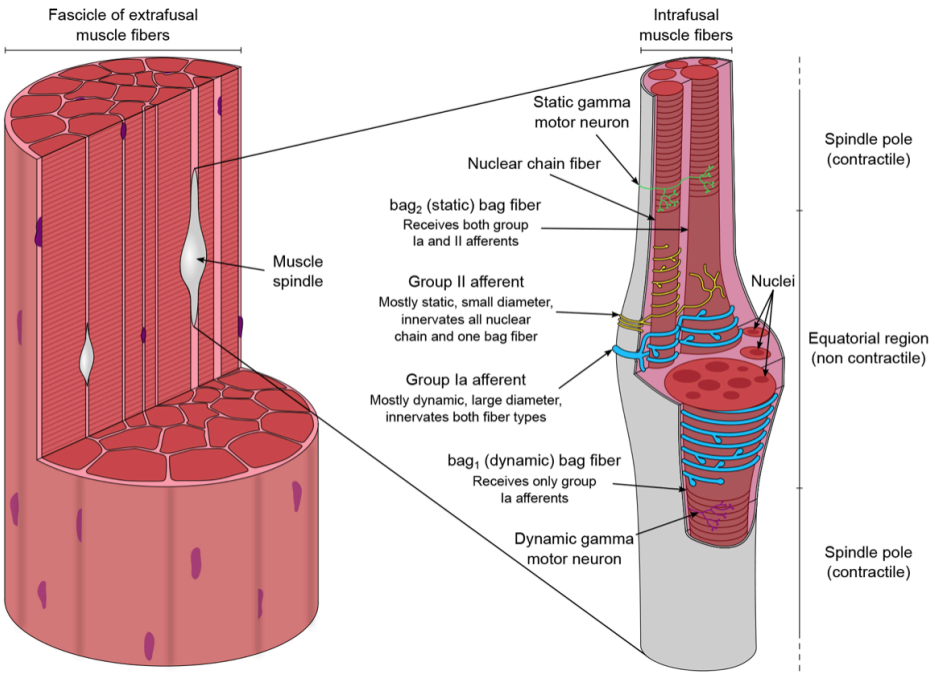

Figure 1: *Morphology of fascicle of extrafusal fibers (on the left) and muscle spindle (right) [1]*

Extrafusal muscle fibers on the outside of the spindle generate force through their contraction. Intrafusal muscle fibers inside the spindle modulate transduction properties without contributing to overall muscle force generation. Muscle spindle consists of contractile fibers in two polar regions flanking a central/equatorial non-contractile zone. This equatorial part can be stretched either during muscle stretch or during contraction of the two striated poles [1]. This leads to activation of sensory endings in the equatorial region responsible for signal transduction. Within the central region of intrafusal muscle fibers there are two fiber types: nuclear bag and nuclear chain. Nuclear bag fibers are longer and larger slow-twitch fibers in diameter which contain a cluster of nuclei, whereas nuclear chain fibers are shorter and thinner fast-twitch fibers containing nuclei in single file. These fibers are innervated by different afferents, or sensory neurons that provide sensory information to the brain. These include either a single group Ia afferent is larger in diameter or several group II afferent which are smaller in diameter, with both entering the spinal cord through the dorsal roots [2].

Although there is one type of nuclear chain fiber, there are two types of nuclear bag fibers. Bag fibers innervated by Group Ia afferents are known as bag_1 nuclear bag fibers and bag fibers that

are innervated by both Group Ia and Group II afferents are known as bag_2 nuclear bag fibers. Bag_1 fibers are also called "dynamic bag fibers" because group Ia afferents respond primarily to the dynamic aspect of muscle stretch. Bag_2 fibers are also called "static bag fibers" because group II afferents primarily respond to the static, steady-state aspect of stretch. Muscle spindle consists of up to eight fibers: two nuclear bag fibers and a number of nuclear chain fibers [3]. Further, the contraction of the polar heads of intrafusal muscle receive beta and gamma efferent innervation. Gamma motor neurons are located in the ventral horn and spinal cord grey matter, with these neurons smaller in cell body and smaller in axon diameter thus possessing slower conduction velocity [1]. Gamma motor neurons can also be divided as either dynamic (reaching only bag_1 fibers) or static (reaching both bag and nuclear chain fibers).

Muscle Spindle Function

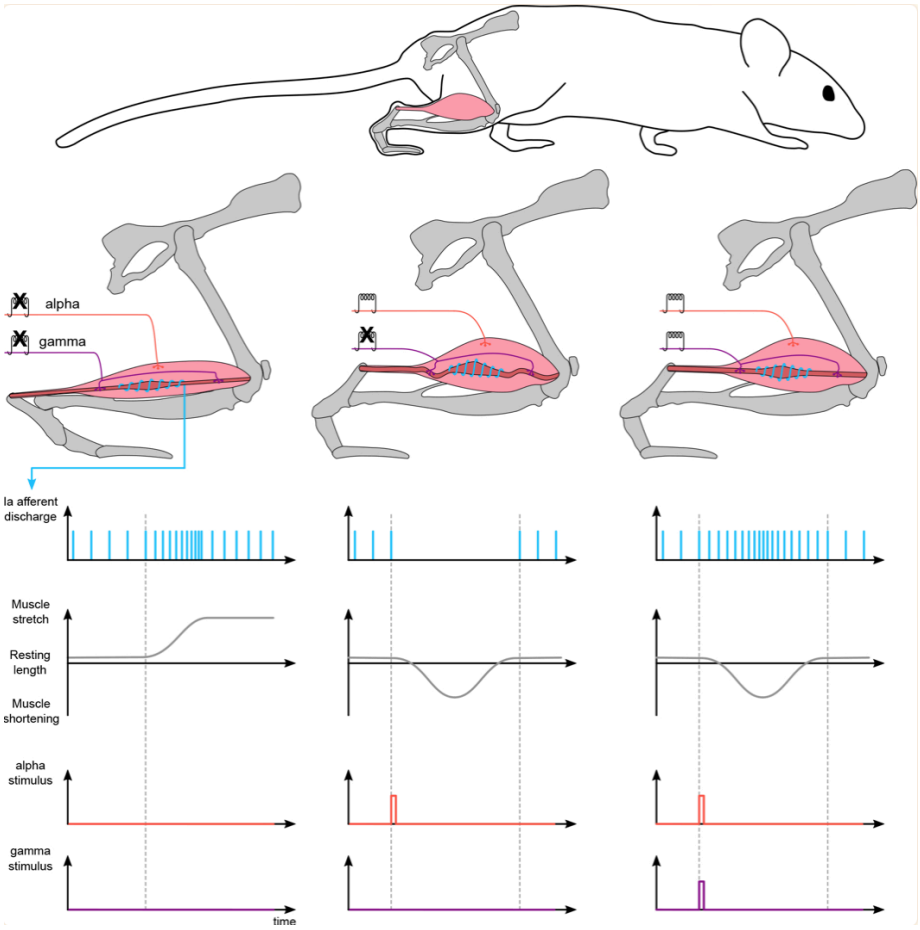

Figure 2: *Diagram showcasing activation of gamma motor neuron maintaining sensitivity of unloaded muscle spindles [1]*

Muscle spindles are specialized sensory organs that detect muscle stretch and contribute to sensation of angular position and movement of joints. Group Ia afferents are influenced by the dynamic aspect of stretch, and these mainly signal angular velocity of joint movement. Group II afferents are affected by static aspects of stretch and thus these signal angular joint position.

When muscle is stretched, primary Ia afferents increase firing rate until steady-state is reached. When muscle is shortened after activation of alpha motor neurons, the muscle spindle unloads and relaxes. Activation of the gamma motor neuron then re-tensions spindle to the extrafusal fibers ensuring transduction capabilities are maintained [1].

Muscle Spindle Physiology

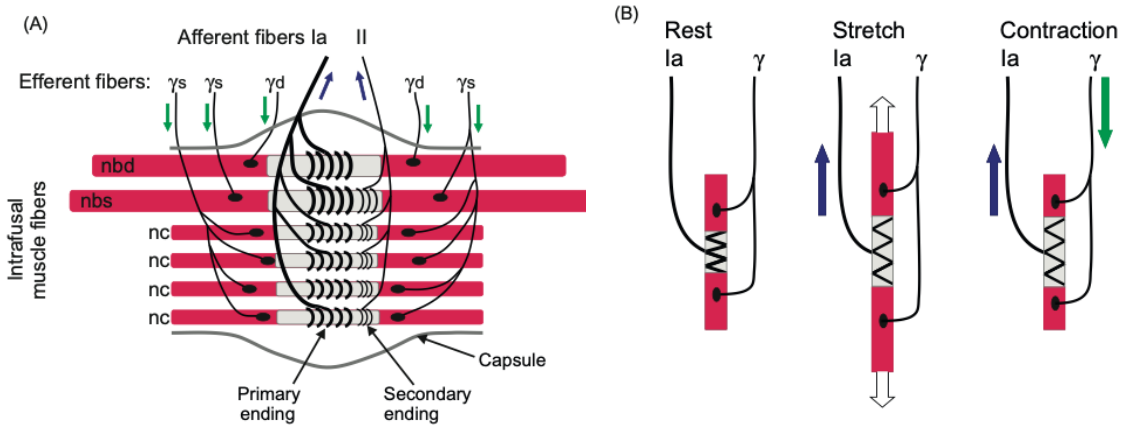

Figure 3: (*A) Muscle spindle structure scheme, (B) muscle stretch and contraction of intrafusal muscle fibers on sensory endings of equatorial region [4]*

Muscle fibers are activated by motoneurons clustered in motor nuclei located in the spinal cord and in the brain stem. The axons of motoneurons travel along nerves to reach target muscles, then branch within the muscle. A motor unit is a complex of one motoneuron and the muscle unit which is a group of innervated muscle fibers. Extrafusal fibers are innervated by large motoneurons either of alpha or beta types, whereas intrafusal muscle fibers are innervated by small gamma type motoneurons as well as by beta motoneurons. Muscle spindles are activated predominately by muscle stretching yielding increase in muscle length and show high sensitivity to stretch. As shown in Figure 3A intrafusal muscle fiber is spirally surrounded by Ia afferent fiber forming the primary ending, able to react to the stretch of each intrafusal muscle fiber. The primary ending is characterized by very high sensitivity and plays a leading role in regulation of muscle activity possessing high frequency bursts of firings in response to increased muscle length during stretch [4]. The primary ending signals the active phase of muscle stretch and when stretching ends and muscle length is maintained the firing rate of Ia afferent fiber decreases.

The sensory ending of type II afferent fiber is called the secondary ending. Secondary endings generate firing rate correlating to change in muscle length but do not change whether the muscle is actively stretched or the length is stable. Thus, secondary endings possess low dynamic sensitivity [4]. As previously mentioned, intrafusal muscle fibers are innervated by gamma and beta motoneurons, further subdivided as either dynamic or static. Dynamic motoneurons (either gamma or beta) innervate only dynamic bag fibers (bag_1). This dynamic bag fiber type moderately increases firing rate of Ia afferent fiber but heavily augments firing burst in response to muscle stretch. Static motoneurons (either gamma or beta) innervate nuclear static bags and/or

nuclear chain fiber, strongly activating both primary and secondary endings. Figure 3B shows muscle stretch and contraction influence on intrafusal muscle fibers on sensory ends. The green arrows point in the direction of conduction of electrical potentials by axons of gamma-motoneurons and the blue arrows point to type Ia and II sensory fibers [4].

Scientific Impact and Motivation

Complete muscle spindle function during movement is still not yet fully understood. Muscle spindle sensory signals are shaped not only by movements of the body but also by motor commands to muscle (alpha drive) and to specialized muscle fibers in muscle spindle mechanosensory region (gamma drive) [1]. However, neuromechanical interactions that lead to muscle spindle firing patterns are still poorly understood, and thus it is necessary to develop a framework for how muscle spindles generate these complex sensory signals during natural movements. Muscle spindle firing is critical in treating neuromuscular disorders and during interactions with devices/interventions to improve motor impairment [2]. Thus, a biophysical modeling approach must be taken to build muscle spindle models based on principles of intrafusal muscle contractile mechanics that can be extended to examine multiscale interactions at the cellular level and in limb mechanics.

‘

Methods

Overview

This novel model outlined by Blum et al. establishes a relationship between muscle spindle firing characteristics and estimated intrafusal fiber force and first time-derivative (yank) in passive stretch conditions [5]. The researchers built a generative model based on a simple representation of intrafusal muscle mechanics. Independent effects of alpha and gamma drive on muscle spindle firing simulated based on mechanical interactions between muscle spindle and muscle-tendon unit.

Coincidently, muscle spindle afferent axonal potentials were recorded and IFRs were computed in experimentally anesthetized rats while stretching the triceps surae muscles. Ia afferent firing rates were recorded from the dorsal rootlets during stretches of the triceps surae muscle. In the relaxed condition (absence of central drive to the muscles) it was assumed that extrafusal muscle fiber forces provided a reasonable estimate for resistive force of the intrafusal muscle fibers within the muscle spindle mechanosensory apparatus [5].

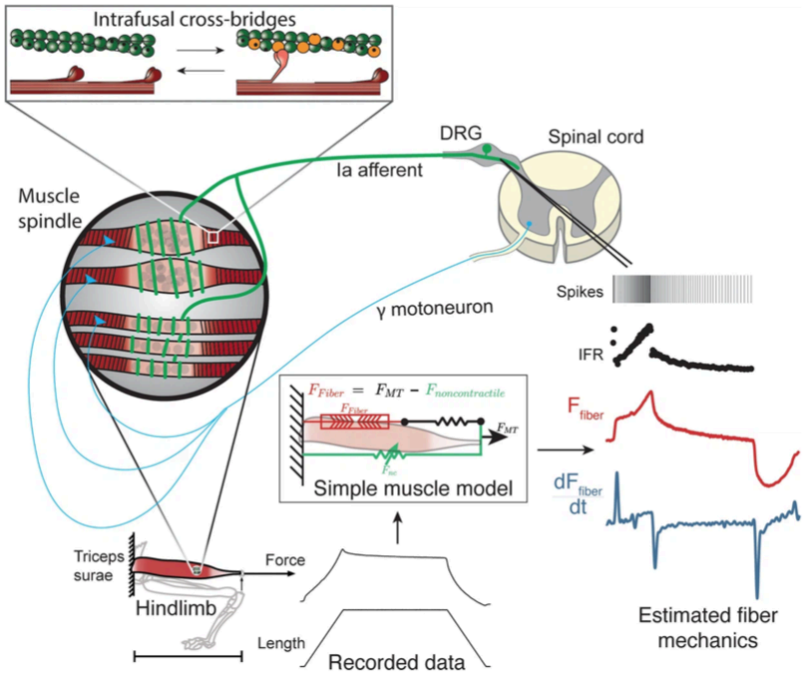

Figure 4: *Methodology overview evaluating hypothesis that muscle spindle Ia afferent firing follows intrafusal muscle fiber force accounted for by cross-bridge interactions [5]*

In Figure 4, the red trace represents the initial rise in extrafusal muscle fiber force at the onset of stretch and the blue trace represents the yank signal yielded, which becomes more apparent once the extracellular tissue forces are subtracted from whole musculotendon force as discussed further [5]. Muscle fiber forces were estimated by subtracting noncontractile forces from the measured whole musculotendon force. The remaining estimated muscle fiber force and yank exhibited similar characteristics to the muscle spindle IFR. Intrafusal muscle fiber force and yank

were then simulated using a cross-bridge based model discussed in further detail to predict muscle spindle IFRs.

Governing Equations and Parameterization

Muscle Spindle Biomechanics Modeling

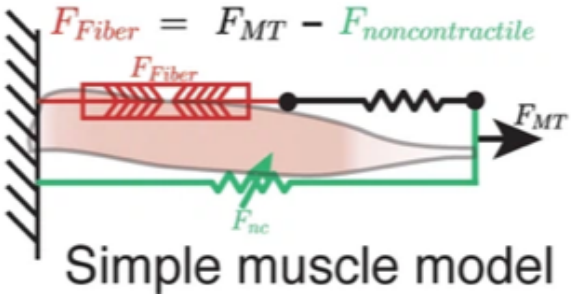

Figure 5: *Simple idealized muscle fiber force model schematic [5]*

Researchers assumed an idealized musculotendon mechanical arrangement to isolate a component of recorded force arising from muscle fibers. The noncontractile passive connective tissue is arranged mechanically in parallel with muscle fibers as seen in Figure 5. The exponential rise in force with stretch was assumed to arise from the non-contractile tissue in parallel with the muscle-tendon unit with exponential stiffness. It is assumed that the noncontractile tissue acted as nonlinear spring of the form [5]:

$$F_{nc} = k_{lin}\,(L - L_0) + Ae^{k_{exp}(L-L_0)}$$

Where k_{lin}, k_{esp}, and A are parameters greater than or equal to zero. The estimated noncontractile tissue forces were subtracted from recorded force to estimate muscle fiber force and were fitted to the instantaneous firing rates (IFR) modeled as further elaborated.

Instantaneous Firing Rate Modeling

Researchers predicted spiking responses using combinations of either recorded musculotendon length-related (length, velocity, and acceleration) or force-related (estimated muscle fiber force and yank) variables, with the weights and offsets for each variable optimized to minimize squared error between model prediction and Ia spike rates.

The estimated IFR for both force and length related models were fitted to the IFR of the afferent for each stretch trial. Model parameters such as weight (k_i) and offset (b_i) for each force- or length-related variable were included in the sum determined by least-squares regression. Time delay was determined accounting for apparent delay between muscle force response and onset of spiking response. The instantaneous firing rate general form for models was as follows [5]:

$$IFR_{j,n}(t) = \left(\sum_{i=1}^{n} k_i \cdot \left(x_i \left(t - \lambda_j \right) + b_i \right) \right)$$

The model estimates for IFR were related to the recorded IFR of the m afferent by the equation [5]:

$$IFR_{j,n}(t) + e(t) = IFR_{m,n}(t)$$

Where the error e(t) was minimized by finding a set of parameters for each model that minimizes measure related to $e(t)^2$.

Intrafusal Muscle Modeling

To simulate hypothesized mechanisms of intrafusal muscle fibers, researchers utilized a computational model of cross-bridge cycling. Researchers implemented this computational model in MATLAB based on this simplified structure of model shown.

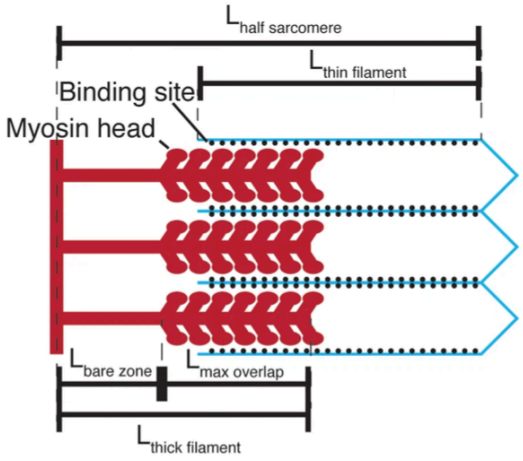

Figure 6: *Schematic of length variables accounted for half sarcomere model [5]*

The researchers focused on thick filament kinetics and greatly simplified thin filament instead of simulated coupled dynamics between myosin heads and actin binding sites. In Figure 6, the overlap between the myosin heads and the actin binding sites is the relevant variable for the simulations. Force in each half sarcomere was calculated as a sum of two components: active component (generated by cycling activity of myosin heads) and passive component (generated by simulated linear spring) as shown [5]:

$$Total\ Force = \int_{-\infty}^{+\infty} \left(k_{cb}\, \rho\, f(x) \ \ \left(x + x_{ps} \right) \ dx \right)$$
$$+ k_{pas} \left(l_{hs} - l_0 \right)$$

The model calculates force of half sarcomere at each time step, adding forces generated from each myosin head attached to actin binding site (the active force) with elastic force of titin (the passive force). The active force is calculated as the fraction of attached myosin heads (f) multiplied by the number density (ρ), unit stiffness of a single attached actin-myosin cross-bridge (k_{cb}), and by the length of the cross-bridges ($x + x_{ps}$) integrated across cross-bridge lengths. The passive force component was calculated as length of the sarcomere (l_{hs}) relative to reference length (l_0) multiplied by linear stiffness (k_{pas}) [5].

The myosin cycling dynamics were modeled using a two-state system in which each myosin head could either be attached as a cross-bridge with length x, or detached. The numbers of myosin heads in each of these states were governed by the system of partial differential equations [5].

$$\frac{\delta A(x,t)}{\delta t} = k_f(x)\,D(t) - k_g(x)\,A(x,t)$$

$$\frac{\delta D(t)}{\delta t} = \int_{-\infty}^{+\infty} k_g(x)\,A(x,t)\,dx - \int_{-\infty}^{+\infty} k_f(x)\,D(t)\,dx$$

where A(x,t) is the number of attached myosin heads attached to actin binding sites at time t extended by length x and D(t) is the number of myosin heads in the detached state. The rate equations $k_f(x)$ and $k_g(x)$ are the forward and reverse rates of myosin attachment and are both functions of cross-bridge length, x. The partial differential equations were simplified into a system of ODEs by solving the time-dependent equations simultaneously at each cross-bridge length [5].

Intrafusal muscle model parameters

Table I: *Intrafusal model constant parameters [5]*

Parameter	Value (dynamic, static fiber)	Units	Description
k_{cb}	1	mN m^{-1}	Unit cross-bridge stiffness
x_{ps}	2.5	nm	Unit power stroke distance
$L_{thick\ filament}$	815	nm	Length of thick filament
$L_{thin\ filament}$	1120	nm	Length of thin filament
$L_{bare\ zone}$	80	nm	Length of bare zone
$c_{filament}$	0.5	-	Filament compliance factor
ρ_{cb}	6.9×10^{16}	m^{-2}	Cross-bridge number density
l_0	1050, 1200	nm	Passive force reference length
k_{pas}	100, 250	N m^{-2} nm^{-1}	Passive force linear stiffness

Table I outlines constant parameters used in both dynamic and static intrafusal muscle fiber models. These parameters did not change in any simulation run and provided values for constants for the computationally constructed half-sarcomere model.

Muscle Spindle Response to Stretch

A combination of force and yank was used to model the transformation of intrafusal muscle fiber stress into a firing waveform. The model consists of a "static" fiber and a "dynamic" fiber based on observations that muscle spindle primary afferent responses to stretch consisting of two components. For these simulations, each muscle fiber model used identical parameters, but the contribution of each fiber to the neural firing rate varied [5]:

$$r(t) = r_{dynamic}(t) + r_{static}(t),$$

The total firing rate of the afferent, r(t), is represented as a sum of the dynamic and static fiber components, or $r_{dynamic}(t)$ and $r_{static}(t)$, respectively. The static component was defined as [5]:

$$r_{static}(t) = k_{Fs} F_s(t),$$

where k_{Fs} is a constant and $F_s(t)$ is the total force in the static fiber. The dynamic component was defined as [5]:

$$r_{dynamic}(t) = k_{Fd} F_d(t) + k_{\dot{F}d} \dot{F}_d(t),$$

where k_{Fd} and $k^{\cdot}_{Fd}$ are constants, and $F_d(t)$ and $F^{\cdot}_d(t)$ are respectively the force and yank of the cycling cross-bridges in the dynamic fiber. Default values for k_{Fs}, k_{Fd}, and $k^{\cdot}_{Fd}$ of 1, 1, and 0.03 were used, respectively [5]. The static and dynamic fibers are arranged in mechanical parallel and were allowed to be activated independently. Thus, the actions of the dynamic and static fibers could be simulated simultaneously or sequentially.

To account for an "occlusive interaction" between dynamic and static branches of the muscle spindle Ia afferent ending, a summation of the static and dynamic components was used as shown [5]:

$$r(t) = f_{occ} r_{dynamic}(t) + r_{static}(t), \quad r_{dynamic} \geq r_{static}$$

$$r(t) = r_{dynamic}(t) + f_{occ} r_{static}(t), \quad r_{static} > r_{dynamic}$$

where f_{occ} is an occlusion factor limiting the contribution of either component to the overall firing rate. This parameter was set to 0.3 (unitless) for all simulations [5].

Results

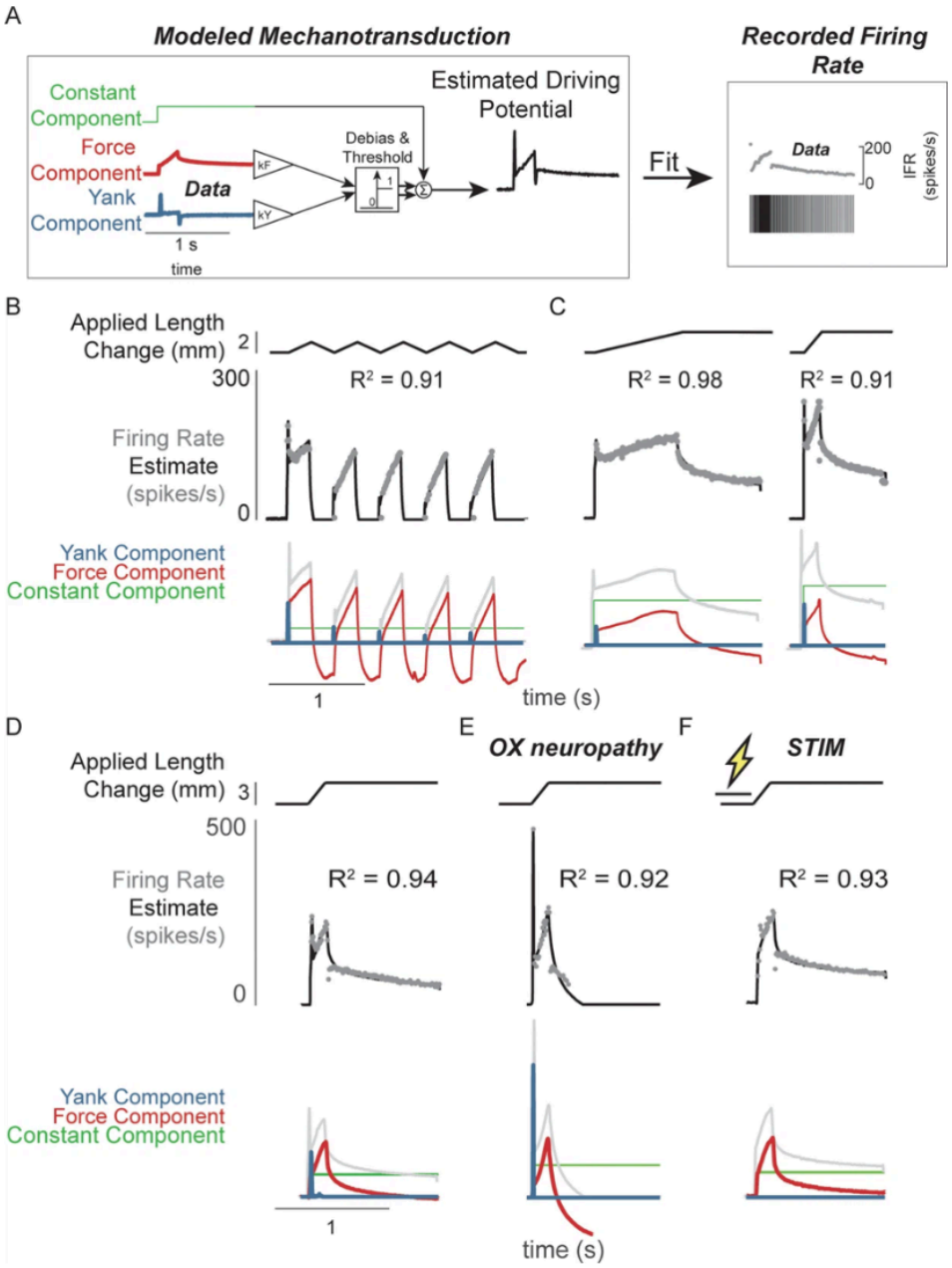

Figure 6: *Muscle spindle potentials estimated from contributions of experimentally-derived muscle fiber force and yank [5]*

In Figure 6A, through combining linear combinations of muscle fiber force and yank, half-wave driving potentials were calculated and compared to the recorded rates of muscle spindle Ia afferent firing. Each component's weight was adjusted to best fit the dynamics of the observed spiking. In Figure 6B, recorded muscle spindle Ia afferent firing rates (gray dots) under history-dependent conditions were replicated (black lines) using muscle fiber force and yank. These firing rates had correlations to muscle length and velocity. Increased muscle fiber yank at

the first stretch and increased firing throughout the ramp were linked to the initial burst and increased force, respectively. In Figure 6C, the temporal dynamics of Ia afferent firing in response to both slow and quick stretches may be explained by muscle fiber force and yank. In Figure D, the force and yank contributions to muscle spindle firing rates can be independently altered using this model. Changed muscle spindle Ia afferent firing patterns are shown attributed to sensory neuropathy generated by oxaliplatin chemotherapy as a loss of force sensitivity in Figure 6E and loss of yank sensitivity following antidromic electrical stimulation of the axon in Figure 6F [5].

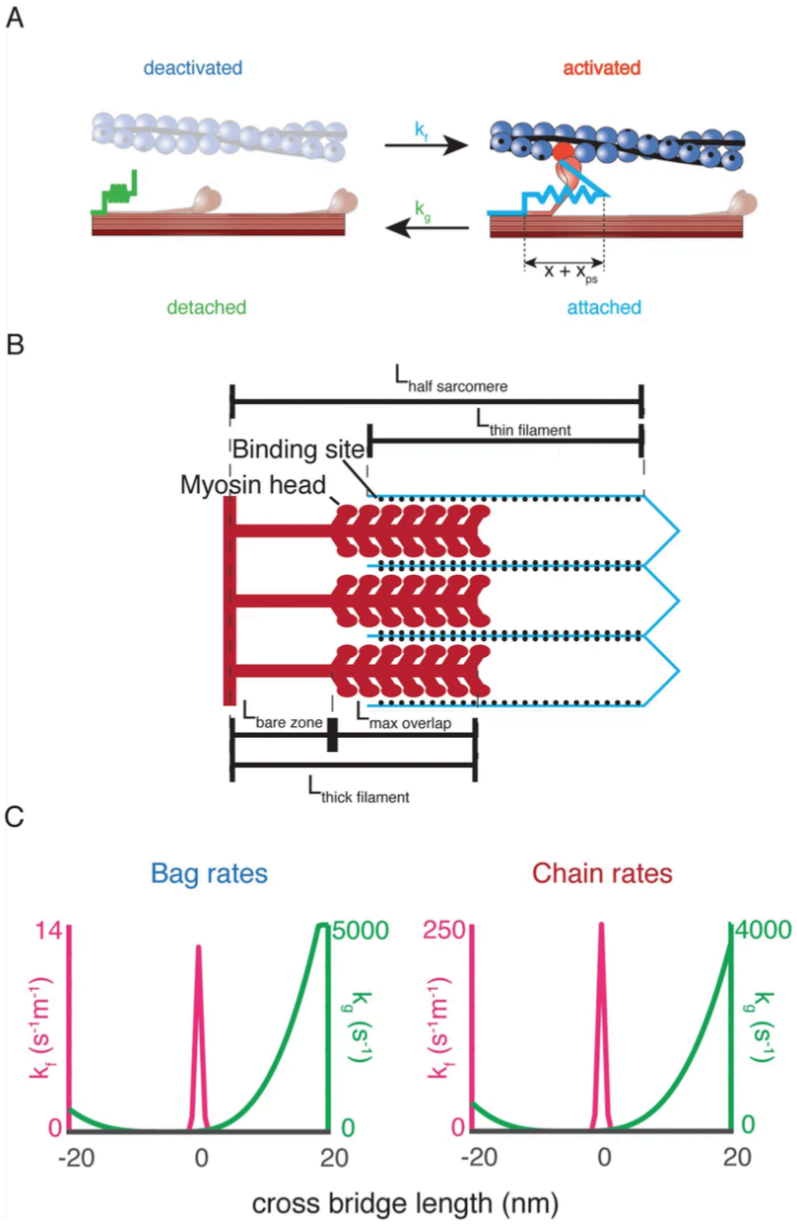

Figure 7: *Biophysical intrafusal muscle model schematic and myosin dynamics [5]*

The cross-bridge cycling two-state dynamic system is shown in Figure 7A. Detachable cross-bridge populations attach at a rate of $k_f(x)$, while attached cross-bridge populations detach at a rate of $k_g(x)$. A contractile force is produced when a cross-bridge with length x is established by applying an extra "powerstroke" length, x_{ps}, to the cross-bridge. Figure 7B displays the schematic of length factors considered in the muscle model. The crucial variable for the simulations is the degree of overlap (black dots) between the thin filament's actin binding sites (blue lines) and the thick filament's myosin heads (red lines). The rate equations for myosin dynamics are displayed in Figure 7C. A Gaussian function with a center at 0 nm, $k_f(x)$ of attachment represents the rate at which detached myosin heads will attach as a function of length (shown in blue). An offset polynomial function (shown in red) determines the rate at which attached cross-bridges will separate as a function of their length, $k_g(x)$ [5].

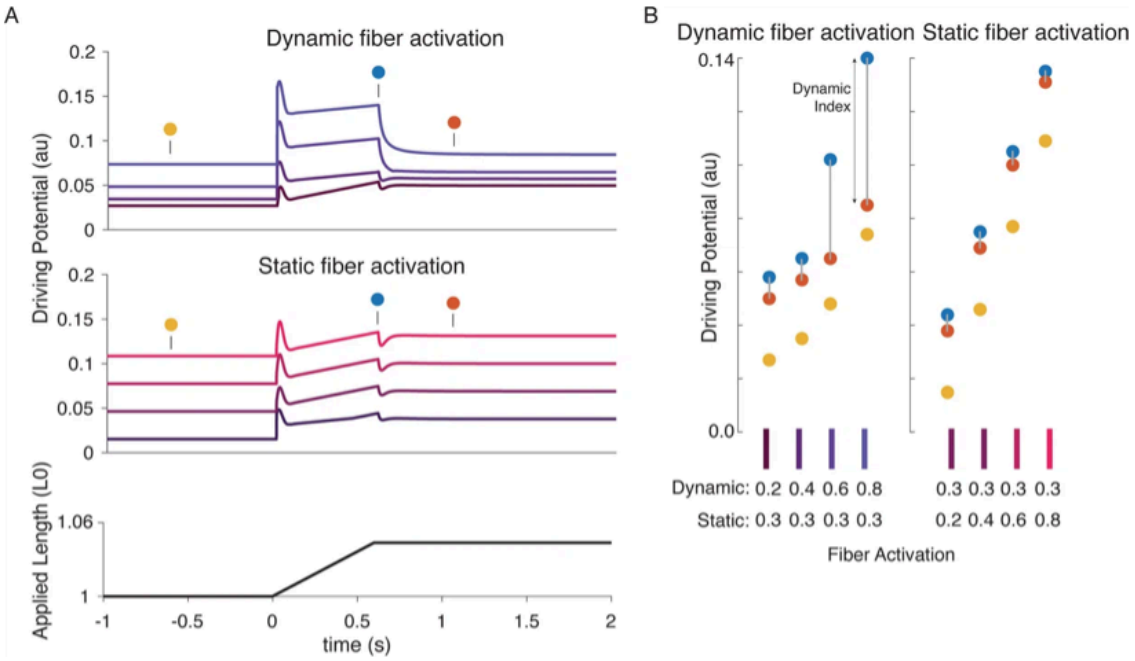

Figure 8: *Change in muscle spindle sensitivity emerging from dynamic and static fiber interactions [5]*

Modifications in the sensitivity of the muscle spindle was resulting from interactions between the dynamic and static fibers and central drive. By increasing the number of active actin binding sites in the corresponding fiber, afferent activity was imposed on either the static or the dynamic fiber [5]. In Figure 8A, the driving potential was mostly increased during the ramp by simulated dynamic fiber activation, with minor increases occurring throughout the background and hold phase (top traces). During the background and hold periods, simulated static fiber activation mostly raises the driving potential rate; during the ramp, increases are only slightly greater. Dynamic index increasing with bag fiber activation and dynamic index decreasing with chain fiber activation, respectively, were the patterns previously documented in the literature. In Figure 8B, emergent scaling of the dynamic index with dynamic (increase in dynamic index) and static fiber activation (decrease in dynamic index) resembled these trends [5].

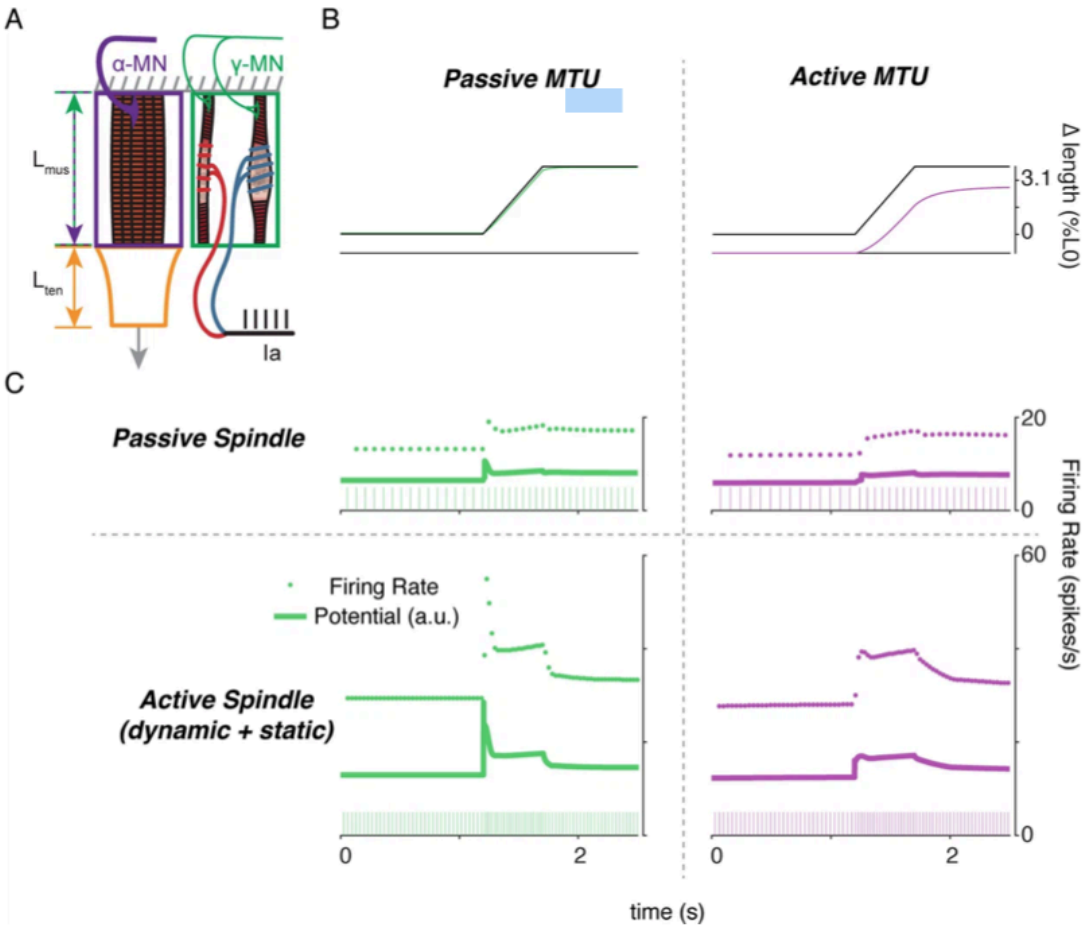

Figure 9: *Analysis of free-end musculotendon simulations [5]*

Muscle spindle Ia firing rates are the result of intricate interactions between movement, alpha, and afferent drive [5]. The framework for free end musculotendon simulations is displayed in Figure 9A. With one end fixed and the other end free to move, an in-series muscle tendon was replicated. The intrafusal muscle fibers, which were triggered separately from the extrafusal muscle, shared the same length as the extrafusal muscle. A muscle-tendon unit (MTU) length change is mostly applied to the muscle, not the tendon, as shown in Figure 9B's passive musculotendon attributed to the muscle's relative compliance. For the same MTU length administered, extrafusal activation results in a relatively rigid muscle, which reduces the length change. The coding characteristics of both passive and active muscle spindles are altered by musculotendon activation, as shown in Figure 9C. A passive muscle spindle experiences an initial burst when the MTU is passive [5].

Discussion and Conclusion

From the novel literature reviewed, it was demonstrated that initially not completely understood Ia afferent firing characteristics are emergent from the muscle contractile cross-bridge mechanisms assessed. Developing a novel simple two-state cross-bridge computational model applying principles of muscle force generation allowed for prediction of nonlinear muscle spindle firing properties, with slow myosin cycling behavior in the dynamic fiber and fast cycling myosin behavior in the static fiber modeled after nuclear bag and chain fiber characteristics, respectively. The dynamic and static motoneuron effects on Ia afferent stretch sensitivity was predicted through application of muscle biophysics. The variations in force and yank sensitivity observed account for the overall firing characteristics as well as the "static-dynamic" variable across the Ia afferents during modeled pass stretch. However, there were shortcomings in the developed model in reproducing the triangle responses from the anesthetized rat model. For example, it may be necessary to replace the simple linear model of titin previously described with more sophisticated properties to capture calcium-dependent regulation of titin stiffness and in muscle force generation. Additionally, researchers failed to account for the complex processes leading to occlusion in transduction within the primary afferent where firing rate may be more dependent on bag_1 fiber during initial stretch and then more dependent upon bag_2 chain fibers in subsequent stretches [5]. Further work could go on to provide a more elaborate muscle fiber model including details about potential neuronal factors regulating spindle firing such as the asymmetrically distributed voltage gated ion channels (VGCs). Asymmetric composition and spatial distribution of these VGCs could impact spindle afferent firing, as they do in neurons in the peripheral, central and autonomic nervous systems [6]. Thus, a computational model built upon muscle cross-bridge model including distribution of VGCs can be reviewed to assess further improved muscle spindle afferent firing mechanics and behavior.

References

[1] Santuz, A., & Akay, T. (2023). Muscle spindles and their role in maintaining robust locomotion. *The Journal of physiology*, *601*(2), 275-285.

[2] Kröger, S., & Watkins, B. (2021). Muscle spindle function in healthy and diseased muscle. *Skeletal Muscle*, *11*(1), 3.

[3] Macefield, V. G., & Knellwolf, T. P. (2018). Functional properties of human muscle spindles. *Journal of neurophysiology*, *120*(2), 452-467.

[4] Celichowski, J., & Krutki, P. (2019). Motor units and muscle receptors. In *Muscle and Exercise Physiology* (pp. 51-91). Academic Press.

[5] Blum, K. P., Campbell, K. S., Horslen, B. C., Nardelli, P., Housley, S. N., Cope, T. C., & Ting, L. H. (2020). Diverse and complex muscle spindle afferent firing properties emerge from multiscale muscle mechanics. *Elife*, *9*, e55177.

[6] Housley, S. N., Powers, R. K., Nardelli, P., Lee, S., Blum, K., Bewick, G. S., ... & Cope, T. C. (2024). Biophysical model of muscle spindle encoding. *Experimental Physiology*, *109*(1), 55-65.